Spectral Coexistence of MIMO Radar and MIMO Cellular System

JASMIN A. MAHAL, Student Member, IEEE
AWAIS KHAWAR
AHMED ABDELHADI, Senior Member, IEEE
T. CHARLES CLANCY, Senior Member, IEEE
Virginia Polytechnic Institute and State University, Arlington, VA, USA

This paper details designing the precoder of a MIMO-radar spectrally-coexistent with a MIMO cellular system. Spectrum sharing with zero or minimal interference is achieved by using, respectively, the conventional switched null space projection (SNSP) or the newly proposed switched small singular value space projection (SSSVSP). Loss in radar target localization capability due to precoding can be compensated by using SSSVSP instead of SNSP to some extent but increasing the number of radar antenna elements is more effective.

Manuscript received January 13, 2016; revised July 6, 2016; released for publication August 22, 2016. Date of publication January 11, 2017; date of current version April 27, 2017.

DOI. No. 10.1109/TAES.2017.2651698

Refereeing of this contribution was handled by F. Gini.

This work was supported by Defense Advanced Research Projects Agency under the SSPARC program. Contract Award Number: HR0011-14-C-0027.

Authors' addresses: The authors are with the Virginia Polytechnic Institute and State University, Arlington, VA 22203, USA, E-mail: (jmahal@vt.edu; awais@vt.edu; aabdelhadi@vt.edu; tcc@vt.edu).

I. INTRODUCTION

Cellular network operators are predicting a 1000 × increase in capacity to keep pace with the tremendous growth of aggregate and per-subscriber data traffic [1]. Increased investments in infrastructure, e.g., larger number of small cells, and more spectrally efficient technologies, e.g., LTE-Advanced, can help meet this challenge partially. The Federal Communications Commission (FCC) is considering a number of options including incentive auctioning and sharing of federal spectrum to meet the commercial spectrum requirements. Of these two, spectrum sharing is a quite promising technology due to the large number of underutilized federal spectrum bands that can be shared with commercial cellular operators to satisfy their growing demands. But spectrum sharing is associated with its inherent set of challenges because the incumbents need to be protected from the harmful interference that can arise due to the operation of other systems in the shared bands.

Spectral coexistence of wireless communication systems and radars is an emerging area of research. Spectrum has been shared in the past primarily between wireless communication systems using opportunistic approaches by users equipped with cognitive radios through spectrum sensing. Although the high UHF radar systems overlap with GSM communication systems, and the S-band radar systems partially overlap with Long Term Evolution (LTE) and WiMax systems, so far, it has not been possible for commercial communication systems, such as WiMAX or LTE, to operate in the vicinity of radar systems on the same or adjacent frequency bands. The high signal power from the radar saturates communication systems receiver amplifiers typically designed to operate at much lower power levels in comparison with radars. This causes outage or interruption of service in communication systems.

In this paper, the authors address the specific problem of spectrum sharing between a multiple-input multiple-output (MIMO) ship-borne defense radar system and a commercial MIMO cellular network consisting of clusters of cooperative base stations (BS), commonly known as coordinated multipoint (CoMP) system. The CoMP system coordinates simultaneous transmissions from multiple BSs to user equipments (UEs) in the downlink and perform joint decoding of UE signals at multiple BSs in the uplink. Thus, the CoMP system utilizes coordination among BSs to effectively turn otherwise harmful intercell interference into useful signals. This results in improved coverage, throughput, and efficiency for over-all cellular system as well as for the cell-edge users. Due to these advantages of the CoMP system over traditional cellular system, 3GPP LTE-Advanced Release 11 and beyond consider CoMP as an enabling technology for 4G mobile systems [2].

Protecting the primary user (PU) or the incumbent Federal user from the harmful interferences from the secondary user (SU) or the commercial user and modifying the SU signal accordingly is the approach adopted by the first two generations of spectrum sharing between a Federal radar and a commercial communication system. In this approach,

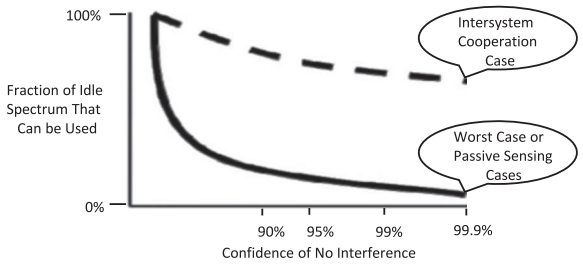

Fig. 1. Fraction of idle spectrum that can be used under different cases [3].

government users are entirely passive as they were not designed for sharing in mind which places the entire burden on commercial system to maintain an extremely high confidence level of interference protection for Federal users. However, the potential for such sharing with very conservative criteria is naturally so limited that this approach has made only modest progress in the U.S. to date [3]. The basic issue is addressed by Marcus as presented in Fig. 1 [3]. The plot shows the percentage of idle spectrum that can be used as a function of the required confidence of no or negligible interference to the PU. If the PU is not designed with any sharing in mind as is the case with current incumbents then interference protections have to consider all possible worst case scenarios. This results in the very conservative sharing criteria. However, if the PU is originally designed with the anticipation of sharing and can cooperate with the new user, then a significantly higher fraction of idle spectrum can be utilized. Consequently, as Marcus suggested a third generation of sharing could be based upon the innovative design of the Federal systems with the intention of sharing.

Moreover, in a Fast Track report by National Telecommunications and Information Administration (NTIA), it was proposed that in order to prevent the burnout or saturation of commercial cellular communication systems from high-powered Federal radar signal, large exclusion zones are required [4]. But these exclusion zones cover a large portion of the U.S. where majority of the population lives and, thus, does not make a business case for commercial deployment in radar bands.

The above-mentioned issues motivated us to think along the line of modifying the PU signal and cooperative sharing between the Federal radar and the commercial communication system. Novelty of our approach lies in the assumption of amicable coexistence of two users both in frequency and time. Typical radar operations only use the frequency bands sporadically both in time and space that presents an interesting opportunity to be exploited by the commercial wireless communication system whose radiation is isotropic and the signal coverage is almost everywhere at all times [5]. Due to the assumption of MIMO structure on both sides, the communication signal can also be precoded so that they are in the null space of the radar. But the Federal radars are inherently robust against interference as they must provide a high degree of suppression for all forms of clutter return. Another option could be precoding on both sides, radar as well as CoMP system. But this choice is theoretically infeasible as explained in proposition 1. Consequently, we choose to do the precoding with the radar rather than the communication system.

Authors in this paper design the radar precoder for two modes of operation: cooperation/cognition mode and interference-mitigation mode. During the cooperation/cognition mode, the radar not only broadcast (BC) information to the communication system using the designed precoder but also, utilizing its sensing capability, the radar collects information about the BS-clusters, estimates the channel either by using training symbols sent by the communication system or by blind null-space learning. By processing these information, the radar decides on the best BS-cluster for NSP/SSVSP during interference-mitigation mode.

A. Related Work

Various schemes have been proposed to share radar spectrum with communication systems. Spectrum sharing schemes based on waveform shaping was first proposed by Sodagari *et al.* [6] in which the radar waveform was shaped in a way so that it was in the null space of interference channel between the radar and a communication system. This scheme was extended to multicell communication systems by Khawar *et al.* [7] in which spectrum was shared between a MIMO radar and an LTE cellular system with multiple BSs. They proposed algorithms to select the interference channel with the maximum null space to project the radar signal onto that null space. Although this paper addressed a more practical scenario with multiple BSs, at any given time it mitigated interference to only one BS, i.e., the station with the maximum nullity. A similar approach was presented by Babaei *et al.* in which radar waveform was shaped to mitigate interference to all the BSs in the network [8]. Other spectrum sharing approaches include cooperative sensing based spectrum sharing where a radar's allocated bandwidth is shared with communication systems [9]–[11], joint communication-radar platforms that are spectrally agile [12], database-aided sensing at communication systems to enable radar spectrum sharing [13], radar systems that form virtual arrays to coexist with communication systems [14], and beamforming approaches at MIMO radars [5].

B. Our Contributions

Building upon the works in [7] and [8], the authors of this paper have extended the solution approach to address a MIMO ship-borne radar and a MIMO commercial CoMP communication system coexistence scenario, which is applicable for the LTE-Advanced system. Our contributions are summarized as follows:

1) *Precoder Design for Interference Mitigation*: In order to mitigate interference to CoMP system we derive two radar precoders using subspace projection methods in this paper. In the first scheme, the radar projects its signals onto the CoMP BS-clusters and selects the cluster with the maximum null space. This scheme is known

as switched null space projection (SNSP) as radar looks for the optimal cluster at each pulse repetition interval (PRI) and, thus, switches among clusters at each PRI depending upon its mission requirements. In the newly proposed second scheme, called switched small singular value space projection (SSSVSP), the projection space has been expanded to include the subspace corresponding to the small nonzero singular values under a specified threshold in addition to the null space. The precoder is designed based on the knowledge of a composite interference channel matrix between the radar and a particular BS-cluster.

2) *Precoder Design for Cooperation/Cognition*: We derive radar precoders for communicating with the CoMP system based on zero forcing (ZF) and minimum mean-square-error (MMSE) criteria. The purpose of this mode is information exchange between the radar and the CoMP system. This mode is further divided into two phases. In the first phase, the radar is in cognition mode to sense the training symbols sent by the communication system to perform channel estimation. The CoMP system also informs the radar of its clustering information through a control channel. Consequently, this first phase is associated with signal design on the CoMP side rather than the radar side. In the second phase, the radar in BC mode informs the CoMP system about which cluster it has selected for interference mitigation. Obviously, the second phase is associated with radar precoder design for effective radar signal detection at the communication system. The cooperation mode is vital for the success of interference mitigation mode coming right after it. Without this sort of information exchange, spectrum sharing would not be successful.
3) *Precoder Performance Analysis*: In order to evaluate the performance of radar precoders, we perform detailed theoretical analysis. Although theories are developed based on the assumption of perfect channel knowledge, simulations are carried out considering channel estimation errors [15]. We look at the target localization and interference mitigation capabilities of the radar precoders. The results indicate that while the precoder nullifies the radar interference to the clusters, it degrades the radar performance by introducing correlation in the probing signals. We show that this performance loss can be compensated for by two means either by increasing the number of radar antennas or by utilizing small singular value space projection (SSVSP) rather than using null-space projection. Our results show that between the two compensation schemes, the former is more effective.

C. Notations

The vectors and matrices are denoted by lower-case and uppercase boldface letters, respectively (e.g., $\mathbf{j}$ and $\mathbf{J}$). The rank, null space, transpose, and Hermitian transpose of $\mathbf{J}$ are represented by rank$\{\mathbf{J}\}$, $\mathcal{N}\{\mathbf{J}\}$, $\mathbf{J}^T$ and $\mathbf{J}^*$, respectively. The subspace spanned by a set of vectors S is denoted by Span$\{S\}$. The N by N identity matrix is presented by $\mathbf{I}_N$. $\|\cdot\|_2$ and $\|\cdot\|_F$ denote L-2 norm and Frobenius norm, respectively. Moreover, $(X)^+ = \max(X, 0)$. For a quick reference, important notations are summarized in Table I.

TABLE I
Table of Notations

Notation	Description
M	Total number of BSs
K	Total number of UEs
$\mathcal{M}_i$	i^{th} BS-cluster
K_i	i^{th} UE-cluster
M_R	Radar transmit/receive antennas
N_{BS}	BS transmit/receive antennas
N_{UE}	UE transmit/receive antennas
$\tilde{\mathbf{H}}_{i,R}$	Composite interference channel between radar and the i^{th} BS-cluster $\mathcal{M}_i$

D. Organization

The remainder of the paper is structured as follows. Section II details the radar/communication system spectral-coexistence model. Design of radar precoder for different operating modes is described in Section III. The newly proposed SSSVSP algorithms are presented in Section IV. Section V analyzes the performance of the designed radar precoders theoretically. Simulation results are explained in Section VI. Section VII concludes the paper with final remarks.

II. RADAR/COMP SYSTEM SPECTRAL-COEXISTENCE MODELS

In this section, we introduce CoMP communication system model, MIMO radar signal model, and our radar-communication system spectrum sharing scenario.

A. Coordinated Multipoint (CoMP) System

The CoMP reception can be mainly characterized into two classes. One is coordinated scheduling and/or beamforming (CoMP-CS) and the other is joint processing/reception (CoMP-JP). We consider the later for this paper. In this class of joint processing/reception, data from a single UE is detected by multiple BSs to improve the detected signal quality and/or cancel actively interference from other UEs. On the other hand, these BSs can serve a single UE as in the CoMP single-user MIMO (CoMP-SU-MIMO) mode, or serve multiple UEs simultaneously as in the CoMP multiuser MIMO (CoMP-MU-MIMO) mode using the same frequency at the same time, as shown in Fig. 2.

We consider a CoMP system with a total of M BSs forming C_T nonoverlapping sets of BSs with i^{th} BS-cluster denoted by $\mathcal{M}_i = \{1, 2, \ldots, m_i, \ldots, M_i\}$, serving a total of K users forming C_T disjointed sets of UEs with i^{th} UE-cluster denoted by $\mathcal{K}_i = \{1, 2, \ldots, k_i, \ldots, K_i\}$, where $i = \{1, 2, \ldots, C_T\}$. As i^{th} BS-cluster is paired with i^{th} UE-cluster, the k_i^{th} UE in i^{th} UE-cluster receives its message from a cluster of M_i BSs $\mathcal{M}_i \subseteq \mathcal{M}$, where $\mathcal{M} = \{1, 2, \ldots, M\}$ or the m_i^{th} BS in i^{th} BS-cluster is provided

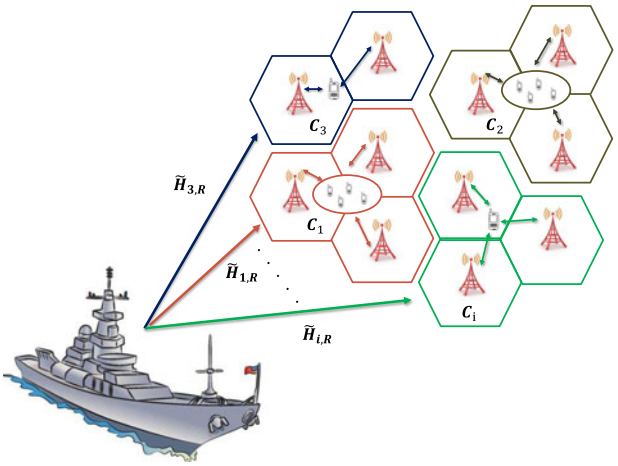

Fig. 2. Spectral coexistence of a littoral MIMO radar (for example, an AN/SPN-43C air traffic control (ATC) radar used by navy in the 3.5-GHz band) with a stationary CoMP system on the shore. An uplink–downlink model
of the CoMP system while sharing radar bands is illustrated.

with the messages of its assigned users set $\mathcal{K}_i \subseteq \mathcal{K}$, where $\mathcal{K} = \{1, 2, \ldots, K\}$. Each BS is equipped with N_{BS} antennas and each UE is equipped with N_{UE} antennas. Consequently, the i^{th} CoMP group consists of M_i cooperative BSs to serve K_i UEs that are paired and jointly scheduled in the same frequency at the same time. In the uplink/downlink, the i^{th} CoMP cluster can form a $(M_i N_{\text{BS}}) \times (K_i N_{\text{UE}})$ virtual MIMO system.

Let $\mathbf{d}_{k_i} \in \mathbb{C}^{N_{\text{UE}} \times 1}$ be the vector of transmit symbols intended for the k_i^{th} UE. All the BSs in the cluster $\mathcal{M}_i$ are informed about the data stream $\mathbf{d}_{k_i}$. This can be realized by utilizing the backhaul links among the BSs and the central switching unit. For user k_i, a linear transmit precoding matrix, $\mathbf{F}_{k_i} \in \mathbb{C}^{M_i N_{\text{BS}} \times N_{\text{UE}}}$, which transforms the data vector $\mathbf{d}_{k_i}$ to the $(M_i N_{\text{BS}} \times 1)$ transmitted vector $\mathbf{F}_{k_i}\mathbf{d}_{k_i}$, is employed by the BSs. The received signal vector $\mathbf{y}_{k_i} \in \mathbb{C}^{N_{\text{UE}} \times 1}$ at the k_i^{th} UE on the downlink is given by

$$\mathbf{y}_{k_i} = \mathbf{G}_{k_i}\mathbf{F}_{k_i}\mathbf{d}_{k_i} + \mathbf{n}_{k_i} \tag{1}$$

where $\mathbf{G}_{k_i} \in \mathbb{C}^{N_{\text{UE}} \times M_i N_{\text{BS}}}$ is the channel matrix between the i^{th} BS-cluster and k_i^{th} user and $\mathbf{n}_{k_i} \in \mathbb{C}^{N_{\text{UE}} \times 1}$ accounts for noise and non-radar interference terms. The network channel for the i^{th} CoMP cluster is defined as $\mathbf{G}_i = [\mathbf{G}_1^T, \mathbf{G}_2^T, \ldots, \mathbf{G}_{K_i}^T]^T$, and the corresponding set of signals received by all K_i users $\mathbf{y}_i \in \mathbb{C}^{K_i N_{\text{UE}} \times 1}$ is expressed by

$$\mathbf{y}_i = \mathbf{G}_i\mathbf{F}_i\mathbf{d}_i + \mathbf{n}_i \tag{2}$$

where $\mathbf{y}_i = [\mathbf{y}_1^T, \mathbf{y}_2^T, \ldots, \mathbf{y}_{K_i}^T]^T$, $\mathbf{F}_i = [\mathbf{F}_1, \mathbf{F}_2, \ldots, \mathbf{F}_{K_i}]$, $\mathbf{d}_i = [\mathbf{d}_1^T, \mathbf{d}_2^T, \ldots, \mathbf{d}_{K_i}^T]^T$, and $\mathbf{n}_i = [\mathbf{n}_1^T, \mathbf{n}_2^T, \ldots, \mathbf{n}_{K_i}^T]^T$. The precoding matrix $\mathbf{F}_i$ is designed based on channel information in order to improve performance of the cooperative-MIMO system.

Similarly, the signal received by the m_i^{th} BS in the i^{th} CoMP cluster $\mathbf{b}_{m_i} \in \mathbb{C}^{N_{\text{BS}} \times 1}$ and the received signal vector at the whole cluster $\mathbf{b}_i \in \mathbb{C}^{M_i N_{\text{BS}} \times 1}$ on the uplink are respectively given by

$$\mathbf{b}_{m_i} = \tilde{\mathbf{G}}_{m_i}\tilde{\mathbf{F}}_{m_i}\mathbf{a}_{m_i} + \tilde{\mathbf{n}}_{m_i} \tag{3}$$

$$\mathbf{b}_i = \tilde{\mathbf{G}}_i\tilde{\mathbf{F}}_i\mathbf{a}_i + \tilde{\mathbf{n}}_i \tag{4}$$

where $\mathbf{a}_{m_i} \in \mathbb{C}^{N_{\text{BS}} \times 1}$ is the signal vector intended for the m_i^{th} BS and $\tilde{\mathbf{n}}_{m_i} \in \mathbb{C}^{N_{\text{BS}} \times 1}$ accounts for the corresponding noise and non-radar interference terms. Moreover, $\tilde{\mathbf{G}}_{m_i} \in \mathbb{C}^{N_{\text{BS}} \times K_i N_{\text{UE}}}$ is the channel matrix between the i^{th} UE-cluster and m_i^{th} BS, and $\tilde{\mathbf{F}}_{m_i} \in \mathbb{C}^{K_i N_{\text{UE}} \times N_{\text{BS}}}$ is the precoding matrix. Also $\tilde{\mathbf{G}}_i = [\tilde{\mathbf{G}}_1^T, \tilde{\mathbf{G}}_2^T, \ldots, \tilde{\mathbf{G}}_{M_i}^T]^T$, $\mathbf{b}_i = [\mathbf{b}_1^T, \mathbf{b}_2^T, \ldots, \mathbf{b}_{M_i}^T]^T$, $\tilde{\mathbf{F}}_i = [\tilde{\mathbf{F}}_1, \tilde{\mathbf{F}}_2, \ldots, \tilde{\mathbf{F}}_{M_i}]$, $\mathbf{a}_i = [\mathbf{a}_1^T, \mathbf{a}_2^T, \ldots, \mathbf{a}_{M_i}^T]^T$, and $\tilde{\mathbf{n}}_i = [\tilde{\mathbf{n}}_1^T, \tilde{\mathbf{n}}_2^T, \ldots, \tilde{\mathbf{n}}_{M_i}^T]^T$. Assuming reciprocity of the channel

$$\tilde{\mathbf{G}}_i = \mathbf{G}_i^*. \tag{5}$$

B. Clustering Algorithms

Joint transmission/reception in the CoMP system requires additional signaling overhead and robust backhaul channels. Due to this reason, only a limited number of BSs cooperate to form a cluster [16]. Cluster formation is an important aspect of the CoMP system in order to exploit benefits promised by the CoMP system. In general, static, and dynamic clustering algorithms are proposed. Each scheme has its own merits that are discussed as follows [17]:

1) *Static Clustering:* Static clusters do not change over time and are designed based on the time-invariant network parameters, such as the geography of BSs and surroundings. As the neighboring BSs interfere the most with each other on average, the clusters are formed by the adjacent BSs only [16].
2) *Dynamic Clustering:* Dynamic clusters continuously adapt to changing parameters in the network, such as UE locations and RF conditions. Dynamic clustering schemes exploit the effect of changing channel conditions, which leads to much higher performance gains without a significant overhead increase [18]. So the dynamic clustering algorithms cluster the BSs not based on their geographical proximity but rather based on their level of interference in the absence of any cooperation [19].

As the narrow radar beam will illuminate a specific geographical area, we use static non-overlapping clustering algorithms with the clusters formed by adjacent cells. We assume that mobile network operators are performing the task of BS clustering and the clustering information is communicated to the radar during the first phase of the cooperation mode.

C. Collocated MIMO Radar

MIMO radar is an emerging area of research and a possible upgrade option of legacy radar systems. Unlike the standard phased-array radar that transmits scaled versions of a single waveform, MIMO radars transmit multiple probing signals that can be chosen freely. This gives MIMO radars significant additional degrees of freedom compared

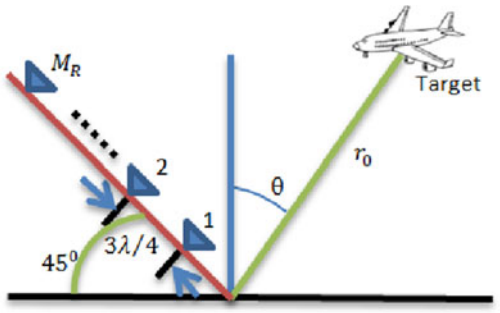

Fig. 3. Configuration of radar antenna array.

to phased-array radars, allowing them to track more targets with better performance, while simultaneously better eliminating clutter and interference. For collocated transmit and receive antennas, the MIMO radar paradigm is shown to offer better target parameter identifiability, and higher spatial resolution [20]–[22] that is very critical for radar operation. For orthogonal signals, MIMO configuration extends the array aperture by virtual sensors. This phenomenon of virtual aperture extension enables MIMO radar to obtain higher DOA estimation accuracy, narrower beams and, therefore, higher angular resolution, and better detection performance.

In this paper, we consider a collocated MIMO radar with equal number of transmit and receive antenna elements, M_R. If we denote the samples of baseband equivalent of M_R-dimensional transmitted radar signals as $\{\mathbf{x}_R(n)\}_{n=1}^{L}$, the signal coherence matrix can be written as [23]

$$\mathbf{R}_{\mathbf{x}} = \frac{1}{L}\sum_{n=1}^{L}\mathbf{x}_R(n)\,\mathbf{x}_R^*(n) = \begin{bmatrix} 1 & \beta_{12} & \dots & \beta_{1M_R} \\ \beta_{21} & 1 & \dots & \beta_{2M_R} \\ \vdots & \vdots & \vdots & \vdots \\ \beta_{M_R1} & \beta_{M_R2} & \dots & 1 \end{bmatrix} \tag{6}$$

where n is the time index, L is the total number of time samples, and β_{oc} denotes the correlation coefficient between o^{th} and c^{th} signals ($1 \le o, c \le M_R$). The phases of the set of correlation coefficients $\{\beta_{oc}\}$, direct the beam to the angle of interest. If $\beta_{oc} = 0$, for $o \ne c$, then $\mathbf{R}_{\mathbf{x}} = \mathbf{I}_{M_R}$, i.e., orthogonal waveforms. This corresponds to omni-directional transmission.

The signal received from a single point target at an angle θ as shown in array configuration in Fig. 3 can be written as [24]

$$\mathbf{y}_R(n) = \alpha\,\mathbf{A}(\theta)\,\mathbf{x}_R(n) + \mathbf{w}(n) \tag{7}$$

where α represents the complex path loss including the propagation loss and the coefficient of reflection and $\mathbf{A}(\theta)$ is the transmit–receive steering matrix defined as

$$\mathbf{A}(\theta) \triangleq \mathbf{a}_t(\theta)\mathbf{a}_r^T(\theta). \tag{8}$$

Denoting the propagation delay between the target and the p^{th} transmit element by $\tau_{t,p}(\theta)$ and the delay between the target and the l^{th} receive element by $\tau_{r,l}(\theta)$, the total propagation delay between the p^{th} transmit element and the l^{th} receive element is given by

$$\tau_{pl}(\theta) = \tau_{t,p}(\theta) + \tau_{r,l}(\theta). \tag{9}$$

Based on these notations of propagation delays, the transmit steering vector, $\mathbf{a}_t(\theta)$ is defined as

$$\mathbf{a}_t(\theta) \triangleq \left[e^{-j\omega_c\tau_{t,1}(\theta)}\cdots e^{-j\omega_c\tau_{t,p}(\theta)}\cdots e^{-j\omega_c\tau_{t,M_R}(\theta)}\right]^T \tag{10}$$

and the receive steering vector, $\mathbf{a}_r(\theta)$ is defined as

$$\mathbf{a}_r(\theta) \triangleq \left[e^{-j\omega_c\tau_{r,1}(\theta)}\cdots e^{-j\omega_c\tau_{r,l}(\theta)}\cdots e^{-j\omega_c\tau_{r,M_R}(\theta)}\right]^T. \tag{11}$$

Using this model, the Cramér Rao Bound (CRB) for target direction estimation is given in (12) [22]. In (12), $\dot{\mathbf{a}}_t(\theta) = \frac{d\mathbf{a}_t}{d\theta}$ and $\dot{\mathbf{a}}_r(\theta) = \frac{d\mathbf{a}_r}{d\theta}$. Assuming all other parameters fixed, the performance of target direction estimation in terms of maximum likelihood (ML) or CRB is optimal for orthogonal probing signals [22], [25], [26].

$$\text{CRB}(\theta) = \frac{1}{2\,\text{SNR}}\left(M_R\dot{\mathbf{a}}_t^*(\theta)\mathbf{R}_{\mathbf{x}}^T\dot{\mathbf{a}}_t(\theta) + \mathbf{a}_t(\theta)^*\mathbf{R}_{\mathbf{x}}^T\mathbf{a}_t(\theta)\right.$$
$$\left.\|\dot{\mathbf{a}}_r(\theta)\|^2 - \frac{M_R\left|\mathbf{a}_t^*(\theta)\mathbf{R}_{\mathbf{x}}^T\dot{\mathbf{a}}_t(\theta)\right|^2}{\mathbf{a}_t^*(\theta)\mathbf{R}_{\mathbf{x}}^T\mathbf{a}_t(\theta)}\right)^{-1}. \tag{12}$$

D. Spectral Coexistence Scenario

The communication system shares the spectrum with a monostatic ship-borne MIMO radar system as shown in Fig. 2. The composite interference channel between radar transmitter and the i^{th} BS-cluster $\mathcal{M}_i$ is denoted by $\tilde{\mathbf{H}}_{i,R} \in \mathbb{C}^{M_i N_{\text{BS}} \times M_R}$. Channels are assumed to be block faded and quasi-static. The signal received by the i^{th} BS-cluster $\mathcal{M}_i$ on the uplink, in the presence of radar, is given simply by

$$\mathbf{b}_i = \tilde{\mathbf{G}}_i\tilde{\mathbf{F}}_i\mathbf{a}_i + \tilde{\mathbf{n}}_i + \tilde{\mathbf{H}}_{i,R}\mathbf{x}_R \tag{13}$$

where $\tilde{\mathbf{H}}_{i,R}\mathbf{x}_R$ is the composite interfering signal from the MIMO radar to the i^{th} BS-cluster that we want to mitigate by designing radar precoders in the next section.

We consider the composite interference channel matrix between the radar and the BS-clusters rather than between the radar and the UEs. The handheld UEs are usually at or near ground level that are expected to communicate with BSs typically located at greater heights than the UEs. The BSs are mounted on the sides of buildings or on building rooftops. As antenna beams for the ship-borne radar systems are tilted somewhat above local horizons, typically about 0.5–1 angular degrees, they will couple more strongly into BS receivers than into the UE receivers as shown schematically in Fig. 4 [27].

III. SIGNAL DESIGN FOR SPECTRAL COEXISTENCE

For amicable spectral coexistence between the radar and the communication system, we design the radar signal so that the interference term, the last term in (13) is forced to zero. The goal is to construct the precoded radar signal $\widetilde{\mathbf{x}}_R$ such that its interference at all of the BSs of the optimally chosen cluster of the CoMP system is either zero-forced or minimized during interference-free mode and the radar keeps switching the beam across the optimal clusters with

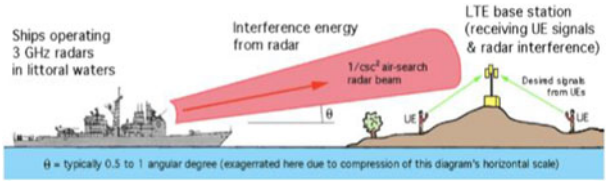

Fig. 4. Schematic diagram showing coupling scenario between littoral radar transmitters and possible future 3.5-GHz LTE systems. By geometry, coupling from radar transmitters should occur more into LTE BS receivers than into UEs [27].

time. For cooperation mode when radar is communicating information to the BSs in the second phase, the radar is precoded to ensure that the bit error rate (BER) of the received signal at the BSs is low enough for effective detection. During the first phase of the cooperation mode, all of the BSs in the cluster coordinate in their choices of training symbols and power transmission so that the radar can estimate the composite interference channel between itself and the BS-cluster optimally.

A. Radar Precoder Design for Interference Mitigation

Radar interference to the i^{th} BS-cluster $\mathcal{M}_i$ can be mitigated by designing the radar precoding matrix $\mathbf{P}_{R,i} \in \mathbb{C}^{M_R \times M_R}$ as

$$\mathbf{H}_{m_i,R}\mathbf{P}_{R,i}\mathbf{x}_R = 0 \quad \forall m_i \in \mathcal{M}_i \tag{14}$$

$$\mathbf{H}_{m_i,R}\widetilde{\mathbf{x}}_R = 0 \quad \forall m_i \in \mathcal{M}_i \tag{15}$$

where the precoded radar signal, $\widetilde{\mathbf{x}}_R = \mathbf{P}_{R,i}\mathbf{x}_R$ and $\mathbf{H}_{m_i,R}$ is the channel matrix between the radar and the m_i^{th} BS in $\mathcal{M}_i$. The above criteria is satisfied by the following condition

$$\mathbf{P}_{R,i}\mathbf{x}_R \in \mathcal{N}\left(\mathbf{H}_{m_i,R}\right) \quad \forall m_i \in \mathcal{M}_i. \tag{16}$$

Therefore, the transmitted radar signal must lie in the null space of $\mathbf{H}_{m_i,R}$ for all m_i. We can rewrite (16) as

$$\mathbf{P}_{R,i}\mathbf{x}_R \in \mathcal{N}\left(\mathbf{H}_{1,R}\right) \cap \mathcal{N}\left(\mathbf{H}_{2,R}\right) \cdots \cap \mathcal{N}\left(\mathbf{H}_{M_i,R}\right). \tag{17}$$

Using the equality $\mathcal{N}(\mathbf{A}) \cap \mathcal{N}(\mathbf{B}) = \mathcal{N}(\mathbf{C})$ where $\mathbf{C} = [\mathbf{A}^*\mathbf{B}^*]^*$, the precoder must satisfy that

$$\mathbf{P}_{R,i}\mathbf{x}_R \in \mathcal{N}\left(\tilde{\mathbf{H}}_{i,R}\right) \tag{18}$$

where

$$\tilde{\mathbf{H}}_{i,R} = \left[\left(\mathbf{H}_{1,R}\right)^*\left(\mathbf{H}_{2,R}\right)^* \cdots \left(\mathbf{H}_{M_i,R}\right)^*\right]^*. \tag{19}$$

To find the null space, we first obtain the singular value decomposition (SVD) of direct communication link [28], which diagonalizes the composite channel matrix $\tilde{\mathbf{H}}_{i,R} \in \mathbb{C}^{M_i N_{\text{BS}} \times M_R}$. The regular form of the SVD of $\tilde{\mathbf{H}}_{i,R}$ is given by $\tilde{\mathbf{H}}_{i,R} = \tilde{\mathbf{U}}_i\tilde{\mathbf{S}}_i\tilde{\mathbf{V}}_i^*$, where $\tilde{\mathbf{U}}_i \in \mathbb{C}^{M_i N_{\text{BS}} \times M_i N_{\text{BS}}}$ is a unitary matrix, $\tilde{\mathbf{S}}_i \in \mathbb{C}^{M_i N_{\text{BS}} \times M_R}$ is a rectangular diagonal matrix with non-negative real numbers on the diagonal, and $\tilde{\mathbf{V}}_i^* \in \mathbb{C}^{M_R \times M_R}$ is another unitary matrix. The diagonal entries of $\tilde{\mathbf{S}}_i$ are known as the singular values of $\tilde{\mathbf{H}}_{i,R}$. The $M_i N_{\text{BS}}$ columns of $\tilde{\mathbf{U}}_i$ and the M_R columns of $\tilde{\mathbf{V}}_i$ are called the left-singular vectors ($\mathbf{u} \in \mathbb{C}^{M_i N_{\text{BS}} \times 1}$) and right-singular vectors ($\mathbf{v} \in \mathbb{C}^{M_R \times 1}$) of $\tilde{\mathbf{H}}_{i,R}$, respectively.

Using SVD, null space of $\tilde{\mathbf{H}}_{i,R}$ is Span$\{\bar{\mathbf{V}}_i\}$ where $\bar{\mathbf{V}}_i$ comprises of the columns of $\tilde{\mathbf{V}}_i$ corresponding to zero singular values of $\tilde{\mathbf{H}}_{i,R}$. The precoder $\mathbf{P}_{R,i}$ is the projection matrix into Span$\{\bar{\mathbf{V}}_i\}$, $\mathbf{P}_{R,i} = \bar{\mathbf{V}}_i(\bar{\mathbf{V}}_i^*\bar{\mathbf{V}}_i)^{-1}\bar{\mathbf{V}}_i^*$.

Assuming that the matrix $\tilde{\mathbf{H}}_{i,R}$ is full row rank, the nullity, i.e., the dimension of null space of $\tilde{\mathbf{H}}_{i,R}$ is greater than the difference metric, $(M_R - M_i N_{\text{BS}})$. In mathematical terms

$$\text{null}\left[\tilde{\mathbf{H}}_{i,R}\right] = \dim\left[\mathcal{N}\left(\tilde{\mathbf{H}}_{i,R}\right)\right] = (M_R - M_i N_{\text{BS}})^+. \tag{20}$$

The necessary condition for a non-trivial precoder ($\mathbf{P}_{R,i} \neq 0$) to exist is that the number of radar transmit antennas is greater than sum of the requested degree of freedom (DoF) of all the BSs in a cluster. In that case, we must have $M_R > M_i N_{\text{BS}}$ to have a nonzero nullity for $\tilde{\mathbf{H}}_{i,R}$ and hence a nonzero precoder.

In SVD, the singular values are always arranged in decreasing order: $\sigma_{M_i N_{\text{BS}}} < \sigma_{M_i N_{\text{BS}}-1} < \cdots < \sigma_1$. These singular values are in fact measures of the transmitted power in the directions of their corresponding right singular vectors. Consequently, projecting the radar transmitted signal onto a space spanned by the right singular vectors corresponding to singular values smaller than a specific threshold σ_{th} will minimize radar interference to the cluster rather than eliminating them completely. This compromise is expected to mitigate the performance loss in radar target detection capability to some extent. The value of σ_{th} is dependent on the power constraints of the communication system. With, $\sigma < \sigma_{\text{th}}$, i.e., when the projection space is formed by the right singular vectors corresponding to the nonzero small singular values under a threshold in addition to the zero singular values, the interference would be reduced to a great extent for the current channel condition. This kind of projection could be called SSVSP. For SSVSP, using SVD of $\tilde{\mathbf{H}}_{i,R}$, the projection space is Span$\{\bar{\mathbf{V}}_{s,i}\}$ where $\bar{\mathbf{V}}_{s,i}$ comprises of the columns of $\tilde{\mathbf{V}}_i$ corresponding to the small nonzero singular values under σ_{th} in addition to the zero singular values. As a result, the precoder $\mathbf{P}_{R_s,i}$ is given by $\mathbf{P}_{R_s,i} = \bar{\mathbf{V}}_{s,i}(\bar{\mathbf{V}}_{s,i}^*\bar{\mathbf{V}}_{s,i})^{-1}\bar{\mathbf{V}}_{s,i}^*$.

Under switched beam condition, the radar keeps scanning for the best composite interference channel between itself and the clusters, and projects its beam toward that cluster. With SNSP, the best and the worst composite interference channels are selected in the following way [7]

$$\tilde{\mathbf{H}}_{\text{best}} = (\tilde{\mathbf{H}}_{i,R})_{i_{\max}} \tag{21}$$

where,

$$i_{\max} = \underset{1 \le i \le C_T}{\arg\max} \dim\left[\mathcal{N}\left(\tilde{\mathbf{H}}_{i,R}\right)\right] \tag{22}$$

and,

$$\tilde{\mathbf{H}}_{\text{worst}} = (\tilde{\mathbf{H}}_{i,R})_{i_{\min}} \tag{23}$$

where,

$$i_{\min} = \underset{1 \le i \le C_T}{\arg\min} \dim\left[\mathcal{N}\left(\tilde{\mathbf{H}}_{i,R}\right)\right]. \tag{24}$$

For newly proposed SSSVSP, the best and the worst composite interference channels are chosen as follows:

$$\tilde{\mathbf{H}}_{\text{best}} = (\tilde{\mathbf{H}}_{i,R})_{i_{\min}} \tag{25}$$

where

$$i_{\min} = \underset{1\le i\le C_T}{\arg\min} \left\| \mathbf{P}_{R_s,i}\mathbf{x}_R - \mathbf{x}_R \right\|_2 \tag{26}$$

and

$$\tilde{\mathbf{H}}_{\text{worst}} = (\tilde{\mathbf{H}}_{i,R})_{i_{\max}} \tag{27}$$

where,

$$i_{\max} = \underset{1\le i\le C_T}{\arg\max} \left\| \mathbf{P}_{R_s,i}\mathbf{x}_R - \mathbf{x}_R \right\|_2 . \tag{28}$$

1) *Singular Value Threshold σ_{th}:* The singular value threshold σ_{th} is determined based on the P_{rad}, which is the allowed radar power level to the communication system so that it does not drive the communication receiver amplifier into saturation. Assuming $\max\{P_{\text{com}}\}$ to be the maximum power allowed at the BS, the corresponding power constraint is given by

$$\begin{aligned} E\left[\left\|\mathbf{P}_{R_s,i}\mathbf{x}_R\right\|^2\right] &= \text{tr}\left\{\mathbf{P}_{R_s,i}\mathbf{P}_{R_s,i}^*\right\} \le \sigma_{\text{th}}^2 P_{\text{rad}} \\ &= \max\{P_{\text{com}}\} \end{aligned} \tag{29}$$

therefore,

$$\sigma_{\text{th}} = \sqrt{\frac{\max\{P_{\text{com}}\}}{P_{\text{rad}}}}. \tag{30}$$

As σ_{th} becomes larger, $\bar{\mathbf{V}}_{s,i}$ approaches $\tilde{\mathbf{V}}_i$ and consequently, $\mathbf{P}_{R_s,i}$ approaches $\mathbf{I}_{M_R}$. Finally, with $\sigma_{\text{th}} \ge \sigma_1$ we have $\bar{\mathbf{V}}_{s,i} = \tilde{\mathbf{V}}_i$ and $\mathbf{P}_{R_s,i} = \mathbf{I}_{M_R}$, which essentially means no precoding at radar with consequent interferences at the communication system but best target detection and localization capability of radar.

2) *Composite Channel Matrix $\tilde{\mathbf{H}}_{i,R}$ and Singular Values:* To make the composite channel matrix full row rank, we assume that the elements of $\tilde{\mathbf{H}}_{i,R}$ are independent, identically distributed and drawn from a continuous Gaussian distribution. According to random matrix theory, this makes the rows of $\tilde{\mathbf{H}}_{i,R}$ linearly independent [29]. Moreover, this also represents the Rayleigh faded multipath environment of typical cellular system. Now as the condition number of composite channel matrix, $Z(\tilde{\mathbf{H}}_{i,R}) = \sigma_{\max}/\sigma_{\min}$ increases, i.e., the more spread out the singular values are, SSSVSP results in less leakage of radar power to the communication system with improved CRB.

B. Radar Precoder Design for Cooperation

In the second phase of this mode, the radar communicates with the CoMP system. The radar informs the communication system of the channel matrices corresponding to BS locations that will be affected by its transmission and the locations that will have a suppressed interference due to the NSP or SSVSP. In this phase, radar operates in BC mode on downlink, i.e., from radar to the BSs. Linear precoding techniques, such as ZF and MMSE precoders, are considered for this MIMO BC mode. By inverting the channel matrix at the transmitter, the ZF precoder can completely eliminate the interference among the BSs. However, a price of high transmission energy has to be paid, especially for near singular matrix channels. This problem can be partially mitigated by using the MMSE linear precoder. This kind of precoder balances the transmission energy and interference level to achieve the minimum detection error. In this mode, radar signal is given by

$$\mathbf{x}_R = [x_{R,1} \ldots x_{R,D_R}]^T \in \mathbb{C}^{D_R}$$

where D_R is the number of independent information streams intended for the BSs and $D_R \le \min(MN_{\text{BS}}, M_R)$. Using ZF criterion, the precoding matrix is given by [30]

$$\mathbf{P}_R = \tilde{\mathbf{H}}_R^* \left(\tilde{\mathbf{H}}_R \tilde{\mathbf{H}}_R^*\right)^{-1} \tag{31}$$

where $\tilde{\mathbf{H}}_R$ is the composite channel between the radar and all the BSs in the communication system and is given by

$$\tilde{\mathbf{H}}_R = \left[(\mathbf{H}_{1R})^*(\mathbf{H}_{2R})^* \cdots (\mathbf{H}_{MR})^*\right]^*. \tag{32}$$

The inverse in (31) can be performed only when the condition, $M_R \ge D_R$, is satisfied. Similarly, using MMSE criterion, the precoder is as follows [31]

$$\mathbf{P}_R = \tilde{\mathbf{H}}_R^* \left(\tilde{\mathbf{H}}_R \tilde{\mathbf{H}}_R^* + D_R\sigma^2\mathbf{I}\right)^{-1}. \tag{33}$$

C. CoMP Signal Design for Interference Mitigation

Due to the assumption of MIMO structure on both sides, the communication signal can also be precoded so that they are in the null space of the radar. If we had done the precoding on the communication side, it would have been performed in the following way. The signal received by the radar while the CoMP system is transmitting on the downlink is given by

$$\mathbf{y}_R(n) = \alpha\, \mathbf{A}(\theta)\, \mathbf{x}_R(n) + \mathbf{w}(n) + \sum_{i=1}^{C_T} \tilde{\mathbf{H}}_{i,R}^* \mathbf{F}_i \mathbf{d}_i \tag{34}$$

where $\tilde{\mathbf{H}}_{i,R}^* \mathbf{F}_i \mathbf{d}_i$ is the composite interfering signal from the i^{th} BS-cluster to the radar which we want to mitigate by designing communication system precoders. As each BS-cluster has its own signal, the goal is to precode the signal of each BS-cluster so that its corresponding interference to the radar is zero. Consequently, each of the C_T interference terms in (34) is forced to zero during interference mitigation mode. This can be realized by designing the associated precoding matrix $\mathbf{F}_i \in \mathbb{C}^{M_i N_{\text{BS}} \times K_i N_{\text{UE}}}$ as

$$\tilde{\mathbf{H}}_{i,R}^* \mathbf{F}_i \mathbf{d}_i = 0. \tag{35}$$

The above criteria is satisfied by the following condition

$$\mathbf{F}_i \mathbf{d}_i \in \mathcal{N}\left(\tilde{\mathbf{H}}_{i,R}^*\right). \tag{36}$$

Therefore, the transmitted communication signal must lie in the left null space of $\tilde{\mathbf{H}}_{i,R}$ for $1 \le i \le C_T$.

1) *Feasibility of null space projection precoding on both radar and communication side:* As MIMO structure is available on both sides, it naturally calls for a possibility of exploiting null-space projection precoding on both sides

so that there is zero mutual interference. The following proposition explains the feasibility of this option.

PROPOSITION 1 *In a spectral coexistence scenario of a MIMO radar and a MIMO communication system, null-space projection precoding to avoid interference is possible on either side but not the both.*

PROOF It is shown in Section III-A that a radar precoder which eliminates its interference to the i^{th} CoMP-cluster, reduces to the projection matrix into null space of an effective interference channel ($\tilde{\mathbf{H}}_{i,R}$). The necessary condition for a non-trivial precoder ($\mathbf{P}_{R,i} \neq 0$) to exist is that the number of radar transmit antennas is greater than sum of the requested DoF of all the BSs in the cluster, i.e., we must have

$$M_R > M_i N_{\text{BS}}.$$

On the other hand, it is shown in Section III-C that the i^{th} CoMP precoder which eliminates its interference to the radar is the projection matrix into the left null space of the effective interference channel ($\tilde{\mathbf{H}}_{i,R}$). The necessary condition for a non-trivial precoder ($\mathbf{F}_i \neq 0$) to exist is that the number of radar transmit antennas is less than sum of the requested DoF of all the BSs in the cluster, i.e., we must have

$$M_R < M_i N_{\text{BS}}.$$

As we end up in contradictory requirements to have null space projection precoding accomplished on both sides, that option is not viable.

D. CoMP Signal Design for Cooperation

In the first phase of this mode the CoMP system basically helps radar in the estimation of $\tilde{\mathbf{H}}_{i,R}$ for all the C_T BS-clusters. We adopt the channel estimation technique as described in [32]. The estimation is carried out by having all the BSs in the i^{th} cluster $\mathcal{M}_i$ send training symbols to the radar and the radar utilizes the received signal to estimate $\tilde{\mathbf{H}}_{i,R}$ and find $\mathbf{P}_{R,i}/\mathbf{P}_{R_s,i}$. As this is a CoMP system, BSs in the i^{th} cluster $\mathcal{M}_i$ can cooperate in their choices of training symbols and transmission power. Further assuming channel reciprocity, the channel from m_i^{th} BS to the radar transmitter is $(\mathbf{H}_{m_i,R})^*$. The composite channel from all of the BSs in the cluster to the radar transmitter is given by

$$\bar{\mathbf{H}}_{i,R} = \left[\left(\mathbf{H}_{1,R}\right)^* \left(\mathbf{H}_{2,R}\right)^* \cdots \left(\mathbf{H}_{M_i,R}\right)^*\right]. \tag{37}$$

We can see that $\tilde{\mathbf{H}}_{i,R} = (\bar{\mathbf{H}}_{i,R})^*$. The coordination among BSs reduces $\bar{\mathbf{H}}_{i,R}$ to a standard MIMO channel. So, by using standard MIMO channel estimation algorithm, the equations for estimation of composite interference channel is as shown below [32]

$$\mathbf{y}_e = \sqrt{\frac{\rho}{M_i N_{\text{BS}}}}\bar{\mathbf{H}}_{i,R}\mathbf{s}_e + \mathbf{w}_e, \quad 1 \leq e \leq L_t. \tag{38}$$

Here L_t is the fixed period at the beginning of each block of L channel uses where the estimation is performed; $\mathbf{y}_e$ and $\mathbf{w}_e$ are, respectively, the M_R-dimensional received signal vector and the noise vector at time e; $\mathbf{s}_e$ is a $(M_i N_{\text{BS}})$-dimensional vector containing the concatenation of training symbols sent by all of the communication BSs in the i^{th} cluster at time e and ρ is the average SNR at each receiving antenna. The ML estimation of the $\bar{\mathbf{H}}_{i,R}$ is given by [32]

$$\hat{\bar{\mathbf{H}}}_{i,R}\,(\text{ML}) = \sqrt{\frac{M_i N_{\text{BS}}}{\rho}}\mathbf{Y}\mathbf{S}^*\left(\mathbf{S}\mathbf{S}^*\right)^{-1} \tag{39}$$

where the matrices are: $\mathbf{Y} = [\mathbf{y}_1\ \mathbf{y}_2\ \cdots\ \mathbf{y}_{L_t}]$, $\mathbf{W} = [\mathbf{w}_1\ \mathbf{w}_2\ \cdots\ \mathbf{w}_{L_t}]$, and $\mathbf{S} = [\mathbf{s}_1\ \mathbf{s}_2\ \cdots\ \mathbf{s}_{L_t}]$. The optimal training symbols that minimizes the mean square error is chosen so that $\mathbf{S}\mathbf{S}^* = L_t\mathbf{I}_{M_i N_{\text{BS}}}$. Cooperation among the BSs is required to choose the optimal training sequence. So, the estimation of $\tilde{\mathbf{H}}_{i,R}$ is given by

$$\hat{\tilde{\mathbf{H}}}_{i,R} = \left[\hat{\bar{\mathbf{H}}}_{i,R}\,(ML)\right]^*. \tag{40}$$

E. Impact of Ship's Motion on Radar Precoder Design

In [33], the Khawar *et al.* investigate this issue and derive coherence time of channel between ship-borne radar and stationary communication system. In addition to ship's horizontal motion (speed), they consider ship's vertical motion (bob) induced by sea and derive the expression for channel coherence time. Considering an AN/SPN-43C ATC radar, used by navy in the 3.5-GHz band, with PRI of 1 ms and mounted on ships that typically move with a top speed of 32 kn, and also assuming the radar transmits fixed-frequency carrier wave pulse modulated waveform and swept-frequency carrier wave pulse modulated waveform (referred to as P0N and Q3N, respectively, in NTIA reports), it is observed that the PRI of radar is much smaller than the coherence time. The coherence time is more than 2.5 ms while the PRIs are 1 ms or less. Therefore, the designed precoder and NSP/SSVSP will be working perfectly even with a moving ship-borne radar without any concerns for CSI being outdated.

F. Two Modes of Operation and the PRI of Radar

The radar will keep switching among two modes of operation and its target detection interval during its pulse repetition interval (PRI $= 1/f_p$) where f_p is the pulse repetition frequency. During the first part of its PRI, it will operate in cooperation/cognition mode for a short period. But this short period is very critical for the proper operation of the radar for the rest of the PRI. In the first phase of the cooperation/cognition mode, it will be basically in cognition mode collecting all the information about the BS clustering of the CoMP and estimating the composite interference channels between itself and the cellular network. The second phase of this mode is associated with the radar informing the communication system of the channel matrices. Based on the vital information it has gathered in the cooperation/cognition mode, it will enter next into the interference-mitigation mode. After this mode, it will remain in its target detection mode for the rest of the PRI. Then the same cycle will repeat as shown in Fig. 5.

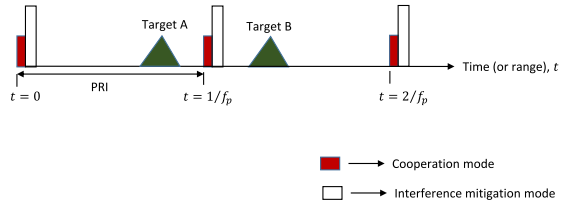

Fig. 5. Schematic diagram presenting the different modes of operation and the PRI of the radar. The cooperation is for brief period to take care of the operational security concerns of the defense radar. The two phases of the cooperation mode are not shown.

Algorithm 1: Optimal Cluster Selection Algorithm.

loop
  for $i = 1 : C_T$ **do**
    Estimate CSI of $\tilde{\mathbf{H}}_{i,R}$.
    Send $\tilde{\mathbf{H}}_{i,R}$ to Algorithm 2 for small singular value space computation.
    Receive $\|\mathbf{P}_{R_s,i}\mathbf{x}_R - \mathbf{x}_R\|_2$ from Algorithm 2.
  end for
  Find $i_{\min} = \arg\min_{1\le i\le C_T} \|\mathbf{P}_{R_s,i}\mathbf{x}_R - \mathbf{x}_R\|_2$.
  Set $\breve{\mathbf{H}} = (\tilde{\mathbf{H}}_{i,R})_{i_{\min}}$ as the best composite interference channel associated with the optimal cluster.
  Send $\breve{\mathbf{H}}$ to Algorithm 2 to get SSVSP radar waveform.
end loop

Algorithm 2: SSVSP Algorithm.

if $\tilde{\mathbf{H}}_{i,R}$ received from Algorithm 1 **then**
  Perform SVD on $\tilde{\mathbf{H}}_{i,R}$ (i.e., $\tilde{\mathbf{H}}_{i,R} = \tilde{\mathbf{U}}_i\tilde{\mathbf{S}}_i\tilde{\mathbf{V}}_i^*$).
  Find SSVSP matrix $\mathbf{P}_{R_s,i} = \bar{\mathbf{V}}_{s,i}\bar{\mathbf{V}}_{s,i}^*$.
  Calculate $\|\mathbf{P}_{R_s,i}\mathbf{x}_R - \mathbf{x}_R\|_2$.
  Send $\|\mathbf{P}_{R_s,i}\mathbf{x}_R - \mathbf{x}_R\|_2$ to Algorithm 1.
end if
if $\breve{\mathbf{H}}$ received from Algorithm 1 **then**
  Perform SVD on $\breve{\mathbf{H}}$ (i.e., $\breve{\mathbf{H}} = \breve{\mathbf{U}}\breve{\mathbf{S}}\breve{\mathbf{V}}^*$).
  Find SSVSP matrix $\breve{\mathbf{P}}_{R_s} = \breve{\mathbf{V}}_s\breve{\mathbf{V}}_s^*$.
  Calculate SSVSP radar signal $\breve{\mathbf{x}}_{R_s} = \breve{\mathbf{P}}_{R_s}\mathbf{x}_R$.
end if

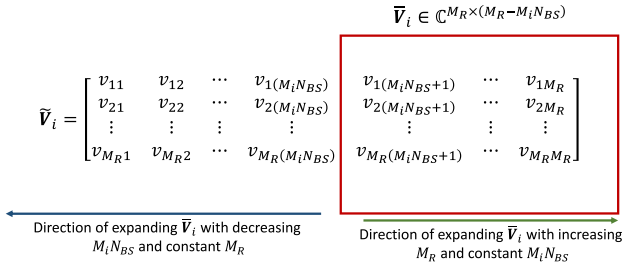

Fig. 6. Schematic diagram presenting how the matrix $\bar{\mathbf{V}}_i$ changes with the variations in M_R, M_i, and N_{BS}. This results in variation in null space with consequent changes in CRB.

IV. SPECTRUM SHARING ALGORITHMS

Based on the background theories presented in Section III-A about the interference-mitigation mode, we propose two new algorithms to implement SSSVSP. As algorithmic implementation of SNSP is already available in the literature [7] and [11], that part is omitted here.

A. Optimal Cluster Selection Algorithm

Our optimal cluster selection algorithm, shown in Algorithm 1, selects the best composite interference channel based on the optimality criteria as mentioned in (25) and (26). Channel state information (CSI)s are obtained using the channel estimation technique as described in Section III-D. The SSVSP projection matrices of all the clusters, available at that time interval are then found using Algorithm 2. Algorithm 2 also calculates the difference between the precoded and the original radar signal and returns it to Algorithm (1). Once Algorithm 1 receives the difference metrics of all the composite interference channels, it selects the best composite interference channel associated with the optimal cluster and sends it to Algorithm 2 for SSVSP radar signal. This is the cognitive algorithm component of the overall system.

B. SSVSP Algorithm

In this section, we present our proposed SSVSP algorithm. On the first cycle, Algorithm (2) gets the CSI estimates of the composite interference channels from Algorithm 1 and finds the corresponding SSVSP matrices using the SVD theorem. It also calculates the associated difference metrics and return them to Algorithm 1. On the second cycle, after receiving the best composite interference channel matrix associated with the optimal cluster from Algorithm 1, it finally calculates the precoded SSVSP radar signal by performing another SVD.

V. THEORETICAL PERFORMANCE ANALYSIS OF THE RADAR PRECODER

This section lays the theoretical foundation of the designed radar precoder performance. As is shown in Section III-A, null space of $\tilde{\mathbf{H}}_{i,R}$ is Span$\{\bar{\mathbf{V}}_i\}$ where $\bar{\mathbf{V}}_i$ comprises of the $M_R - M_iN_{\text{BS}}$ right-most columns of $\tilde{\mathbf{V}}_i$ corresponding to zero singular values of $\tilde{\mathbf{H}}_{i,R}$. As $\tilde{\mathbf{V}}_i$ is a unitary matrix, columns of it form an orthonormal set and rows of it also form an orthonormal set. This results in $\bar{\mathbf{V}}_i$ consisting of a set of orthonormal columns but a set of non-orthonormal rows because the rows of the $\bar{\mathbf{V}}_i$ are actually part of the orthonormal rows of the corresponding unitary matrix as shown in Fig. 6. Consequently, the precoding matrix $\mathbf{P}_{R,i}$ reduces from $(\bar{\mathbf{V}}_i(\bar{\mathbf{V}}_i^*\bar{\mathbf{V}}_i)^{-1}\bar{\mathbf{V}}_i^*)$ to $(\bar{\mathbf{V}}_i\bar{\mathbf{V}}_i^*)$ because being the correlation matrix of the orthonormal columns, $(\bar{\mathbf{V}}_i^*\bar{\mathbf{V}}_i) = I_{M_R-M_iN_{\text{BS}}}$.

On the other hand, being the correlation matrix of the non-orthonormal rows of $\bar{\mathbf{V}}_i$, the precoding matrix comprises of real diagonal elements but nonzero off-diagonal elements. This turns the orthogonal original radar signal $\mathbf{x}_R$ into non-orthogonal precoded radar signal $\tilde{\mathbf{x}}_R$. Although

this precoder eliminates the radar interference to all the BSs in the i^{th} cluster $\mathcal{M}_i$, it affects the spatial correlation of radar probing signals and change their coherence matrix from an identity matrix into one with nonzero off-diagonal elements. For precoded radar signal, the coherence matrix, $\mathbf{R}_{\mathbf{x},i} = E[\widetilde{\mathbf{x}}_R\widetilde{\mathbf{x}}_R^*] = \mathbf{P}_{R,i}E[\mathbf{x}_R\mathbf{x}_R^*]\mathbf{P}_{R,i}^* = \mathbf{P}_{R,i}\mathbf{P}_{R,i}^*$ as $E[\mathbf{x}_R\mathbf{x}_R^*] = I_{M_R}$.

Fig. 6 also reflects the fact that as $M_R - M_iN_{\text{BS}}$ increases with decreasing M_iN_{BS} keeping M_R constant, the rows of $\bar{\mathbf{V}}_i$ approach closer to the orthonormality as it covers more elements of the rows of the corresponding unitary matrix. As a result, the wider null space with more orthonormal row vectors results in less correlated precoded radar signal with consequent improvement in CRB. Same series of events occurs as $M_R - M_iN_{\text{BS}}$ increases with increasing M_R keeping M_iN_{BS} constant. With SSVSP, the $\bar{\mathbf{V}}_i$ gets expanded into $\bar{\mathbf{V}}_{s,i}$ in a similar way. $\bar{\mathbf{V}}_{s,i}$ has more columns and greater part of the rows of the $\tilde{\mathbf{V}}_i$ as compared to $\bar{\mathbf{V}}_i$, which results in improved CRB as compared to NSP.

VI. SIMULATION RESULTS

In this section, the performance of MIMO radar is compared in terms of CRB for target direction estimation with and without radar precoder and as a function of number of antennas per BS, number of BSs per cluster, and number of radar antennas with either SNSP or SSVSP. We have also explored the effect of null-space estimation error on target direction estimation and radar interference to clusters. The distance of target to radar array and the radar interelement spacing are assumed to be $r_0 = 5$ km and $3\lambda/4$, respectively. The frequency of operation is 3.5 GHz. The signal-to-noise ratio between the radar and its target is denoted by SNR while the same parameter between the radar and the cluster of BSs of CoMP system is represented by ρ. The target direction is assumed to be at $\theta = 0^\circ$.

A. Performance Analysis of Interference Mitigating Precoder

Fig. 7 shows the radar CRB performance for orthogonal radar signals as well as precoded radar signals for NSP and SSVSP with estimated CSI. The figure reflects the fact that SSVSP performs better than NSP from the perspective of radar target detection capability as predicted. This plot also shows that as N_{BS} increases, the target localization performance of radar degrades. Because with the increase in N_{BS}, $(M_R - M_iN_{\text{BS}})$ decreases for constant M_R and M_i. So, null space of $\tilde{\mathbf{H}}_{i,R}$ shrinks with consequent impact on the precoder which in turn degrades CRB(θ).

In Fig. 8, we investigate the effect of number of radar antennas (M_R) on the CRB performance of radar. As obvious from (12) that CRB explicitly depends on M_R and improves when M_R increases. For precoded radar signals, increase in M_R leads to increase in the nullity of $\tilde{\mathbf{H}}_{i,R}$ which impacts the choice of $\mathbf{P}_{R,i}$ and results in improved CRB performance. Results in this plot indicate that increasing the number of radar antennas can compensate for the performance degradation in target direction estimation due to correlation in the precoded radar signals. Consequently, for a given target RMSE, number of radar antennas must increase when radar employs a precoder to zero-force or minimize its interference at the BS-clusters.

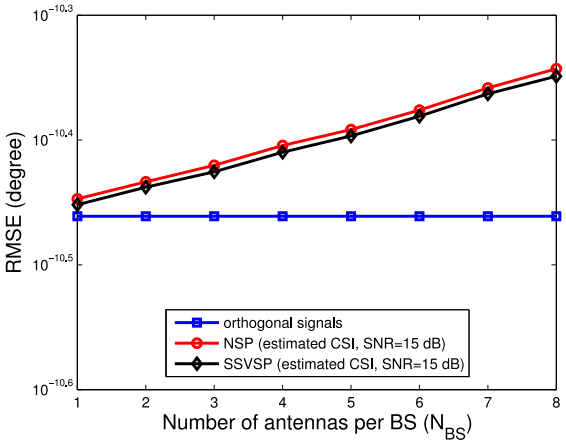

Fig. 7. CRB on direction estimation of the target as a function of antennas employed by the BS when using NSP and SSVSP in a spectrum sharing scenario between MIMO radar and cellular system. A cluster size of $M_i = 3$ is used while having $M_R = 100$ radar antenna elements.

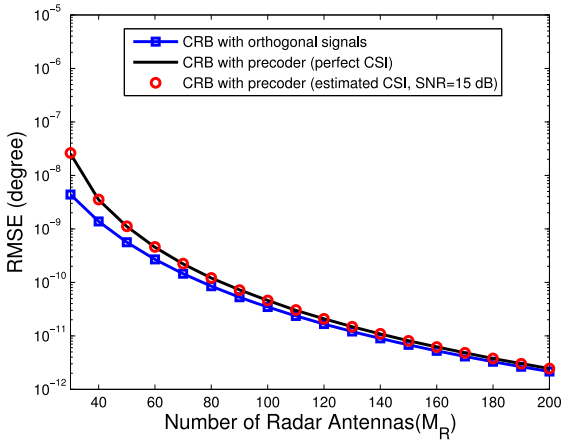

Fig. 8. Effect of number of radar antennas (M_R) on the CRB(θ) performance of radar. A cluster size of $M_i = 3$ is used and $N_{\text{BS}} = 8$.

In Fig. 9, the effect of interference at the clusters is measured using the Frobenius metric, $\sum_{m_i=1}^{M_i}\|\mathbf{H}_{m_i,R}\mathbf{P}_{R,i}\|_F$. Interference becomes less significant as the duration of training phase, L_t increases while it will be completely eliminated with perfect knowledge of $\tilde{\mathbf{H}}_{i,R}$. So, estimated CSI approaches perfect CSI as L_t increases. This plot also reflects the fact that from the perspective of interference at the clusters, NSP outperforms SSVSP to a great extent. With NSP, as M_i increases, $(M_R - M_iN_{\text{BS}})$ decreases for constant M_R and N_{BS}. So, null space of $\tilde{\mathbf{H}}_{i,R}$ shrinks monotonically with consequent monotonic increase in interference at the communication system. With SSVSP, to keep the interference minimum at the communication system, we performed the simulation expanding the null space always by incorporating sub-space corresponding to the smallest singular value. Consequently, as M_i increases keeping M_R and N_{BS} constant, we ended up having gradually de-

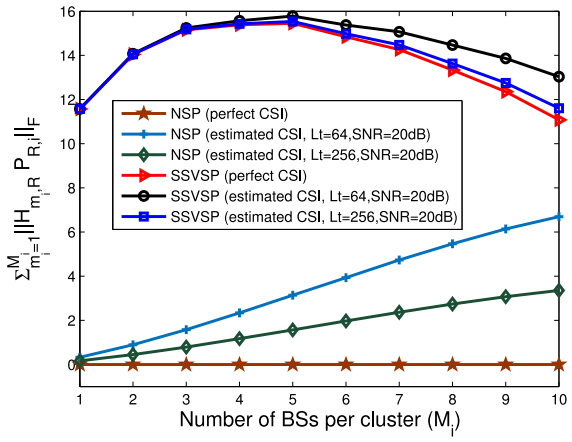

Fig. 9. Variation of radar interference on BS-clusters with cluster size (M_i). $N_{\mathrm{BS}} = 6$ BS antenna elements are used while having $M_R = 100$ radar antenna elements.

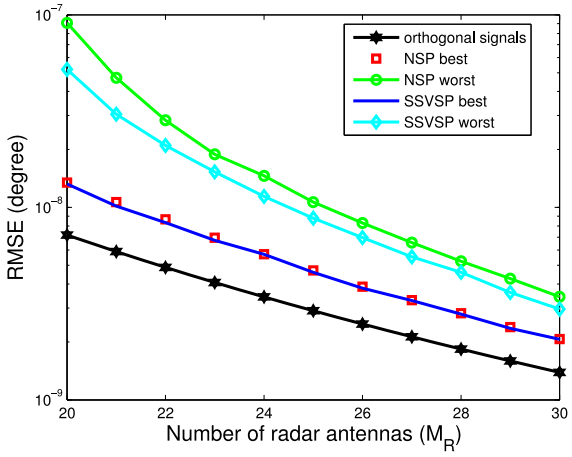

Fig. 10. CRB on direction estimation of the target as a function of number of antenna elements employed by the radar (M_R) with switched NSP and SSVSP while in a spectrum sharing scenario between MIMO radar and cellular system. A cluster size of $M_i = 3$ is used while having estimated CSI. Radar beam is swept across four clusters ($C_T = 4$) and the nullity of the clusters is varied by varying the number of antenna elements per BS, $[N_{\mathrm{BS}} = \{6, 5, 4, 3\}]$.

creasing smallest singular value which in turn led to monotonically decreasing interference leakage to the communication system. The concave curve reflect the fact that as M_i increases, up to certain point gradual shrinking of null space dominates over monotonic decrease in smallest singular value with consequent increase in interference. After that with further increase in M_i, the decrease in smallest singular value dominates over gradual shrinking of null space with consequent decrease in interference.

Fig. 10 plots radar target estimation capability with switched NSP and SSVSP. It is obvious that both of the beam-sweeping methods improve radar performance when the beam is projected on to the optimal cluster associated either with the maximum null space or minimum deviation of the precoded radar signal from the original one. For the worst case scenarios, SSVSP outperforms NSP.

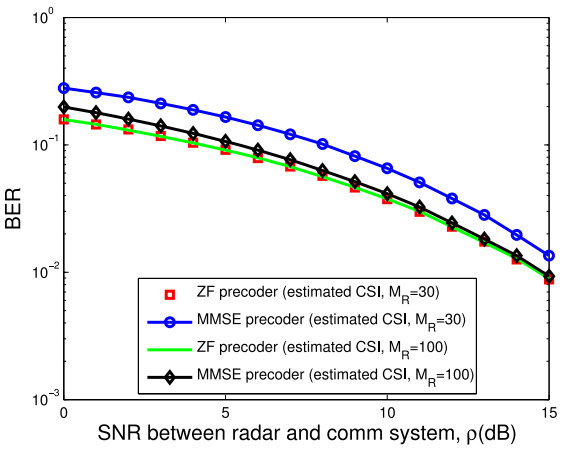

Fig. 11. BER performance during cooperation mode using QPSK waveform. A total of four BSs ($M = 4$) is used.

B. Performance Analysis of Information Exchange Precoder

Fig. 11 shows the spectrum sharing scenario during the second phase of the cooperation mode. The plot represents the performance of the communication system in terms of BER. During simulations, we make sure that $M_R \geq D_R$ that results in non-singular channel matrices. Consequently, ZF outperforms MMSE precoding. The increase in the number of radar antenna is the obvious solution to close the gap between the performance of these two precoding methods.

VII. CONCLUSION

In this paper, the authors design precoders of a ship-borne defense radar in a scenario where a MIMO radar coexists spectrally with a CoMP commercial communication system. We investigate the design of precoder for two modes of radar operation: interference-mitigation mode, when the radar attempts to avoid interference with the communication system and cooperation/cognition mode, when it exchanges information with the CoMP system. For the interference-mitigation mode, the radar steers its beam toward the optimal clusters of BSs and keeps switching the beam from one optimal cluster to another. In case of traditional SNSP, the optimality is decided upon the maximum nullity of the BS-cluster. A new space projection and switching method has been proposed where the beam is steered to the small singular value space of the optimal cluster whose optimality is chosen based on the minimum difference between the precoded and original radar signal. SSSVSP proves to perform better in terms of sacrificing the radar's target localization ability by intentionally allowing some leakage of radar power in the direction of communication system within the power constraints of preventing the communication system from burnout or saturation.

For the second phase of the cooperation mode, the radar precoder is designed based on the ZF and MMSE criteria to reduce BER at the BSs for effective detection. Channel estimation error is taken into account for both modes of operation. Although the introduction of precoding at the radar

tries to mitigate the radar interference at the BS-clusters during interference-free mode, in doing so it causes the radar probing signals lose their orthogonality with consequent performance loss in radar's target parameter estimation capability. SSSVSP mitigates that effect to some extent but increase in the number of radar antenna elements has stronger impact.

Moreover, by modifying the incumbent's signal rather than the SU, we attempted to push out the boundaries of the traditions of the first two generations of spectrum sharing. We tried to tread our own path by designing the future federal systems to enable and actively facilitate more efficient spectrum sharing. This increased sharing could in turn stimulate new economic growth.

ACKNOWLEDGEMENTS

The views, opinions, and/or findings contained in this article/presentation are those of the author(s)/presenter(s) and should not be interpreted as representing the official views or policies of the Department of Defense or the U.S. Government.

REFERENCES

[1] W. Lehr
Toward more efficient spectrum management
MIT Commun. Futures Program, pp. 1–31, Mar. 2014. [Online]. Available: http://cfp.mit.edu/groups/spectrum-policy.shtml

[2] 4G Americas
4G mobile broadband evolution: 3GPP Release 11 & Release 12 and beyond, 2014.

[3] M. J. Marcus
New approaches to private sector sharing of federal government spectrum
New Amer. Found., no. 26, pp. 1–8, Jun. 2009.

[4] NTIA
An assessment of the near-term viability of accommodating wireless broadband systems in the 1675-1710 MHz, 1755-1780 MHz, 3500-3650 MHz, and 4200-4220 MHz, 4380-4400 MHz bands Tech. Rep., Nat. Telecommun. Inf. Admin., Oct. 2010.

[5] H. Deng and B. Himed
Interference mitigation processing for spectrum-sharing between radar and wireless communications systems
IEEE Trans. Aerosp. Electron. Syst., vol. 49, no. 3, pp. 1911–1919, Jul. 2013.

[6] S. Sodagari, A. Khawar, T. C. Clancy, and R. McGwier
A projection based approach for radar and telecommunication systems coexistence
In *Proc. 2012 IEEE, Global Commun. Conf.*, Dec. 2012, pp. 5010–5014.

[7] A. Khawar, A. Abdel-Hadi, and T. C. Clancy
Spectrum sharing between S-band radar and LTE cellular system: A spatial approach
In *Proc. 2014 IEEE Int. Symp. Dyn. Spectrum Access Netw.: SSPARC Workshop*, McLean, VA, USA, Apr. 2014, pp. 7–14.

[8] A. Babaei, W. H. Tranter, and T. Bose
A nullspace-based precoder with subspace expansion for radar/communications coexistence
In *Proc. Globecom 2013—Signal Process. Commun. Symp.*, 2013, pp. 3487–3492.

[9] L. S. Wang, J. P. McGeehan, C. Williams, and A. Doufexi
Application of cooperative sensing in radar-communications coexistence
IET Commun., vol. 2, pp. 856–868, 2008.

[10] M. Ghorbanzadeh, A. Abdelhadi, and T. C. Clancy
A utility proportional fairness resource allocation in spectrally radar-coexistent cellular networks
In *Proc. IEEE Mil. Commun. Conf.*, Oct. 2014, pp. 1498–1503.

[11] H. Shajaiah, A. Khawar, A. Abdel-Hadi, and T. C. Clancy
Resource allocation with carrier aggregation in LTE Advanced cellular system sharing spectrum with S-band radar
In *Proc. IEEE Int. Symp. Dyn. Spectrum Access Networks: SSPARC Workshop*, McLean, VA, USA, Apr. 2014, pp. 34–37.

[12] M. P. Fitz, T. R. Halford, I. Hossain, and S. W. Enserink
Towards simultaneous radar and spectral sensing
In *Proc. IEEE Int. Symp. Dyn. Spectrum Access Netw.*, Apr. 2014, pp. 15–19.

[13] F. Paisana, J. P. Miranda, N. Marchetti, and L. A. DaSilva
Database-aided sensing for radar bands
In *Proc. IEEE Int. Symp. Dyn. Spectrum Access Netw.*, Apr. 2014, pp. 1–6.

[14] C. Shahriar, A. Abdelhadi, and T. Clancy
Overlapped-MIMO radar waveform design for coexistence with communication systems
In *Proc. IEEE Wireless Commun. Netw. Conf.*, Mar. 2015, pp. 223–228.

[15] A. Khawar, A. Abdel-Hadi, and T. C. Clancy
On the impact of time-varying interference-channel on the spatial approach of spectrum sharing between S-band radar and communication system
In *Proc. IEEE Mil. Commun. Conf.*, 2014, pp. 807–812.

[16] F. Boccardi and H. Huang
Limited downlink network coordination in cellular networks
In *Proc. IEEE 18th Int. Symp. Pers., Indoor Mobile Radio Commun.*, Sep. 2007, pp. 1–5.

[17] P. Marsch and G. P. Fettweis, Eds.
Coordinated Multi-Point in Mobile Communications: From Theory to Practice. Cambridge, U.K.: Cambridge Univ. Press, 2011.

[18] A. Papadogiannis, D. Gesbert, and E. Hardouin
A dynamic clustering approach in wireless networks with multi-cell cooperative processing
In *Proc. IEEE Int. Conf. Commun.*, 2008, pp. 4033–4037.

[19] A. Papadogiannis and G. C. Alexandropoulos
The value of dynamic clustering of base stations for future wireless networks
In *Proc. IEEE Int. Conf. Fuzzy Systems*, Jul. 2010, pp. 1–6.

[20] I. Bekkerman and J. Tabrikian
Spatially coded signal model for active arrays
In *Proc. 2004 IEEE Int. Conf. Acoust., Speech, Signal Process.*, vol. 2, Mar. 2004, pp. ii/209–212.

[21] D. W. Bliss and K. W. Forsythe
Multiple-input and multiple-output radar and imaging: Degrees of freedom and resolution
In *Proc. 37th Asilomar Conf. Signals, Syst., Comput.*, vol. 1, Nov. 2003, pp. 54–59.

[22] J. Li and P. Stoica, Eds.
MIMO Radar Signal Processing. Hoboken, NJ, USA: Wiley, 2009.

[23] A. Khawar, A. Abdel-Hadi, T. C. Clancy, and R. McGwier
Beampattern analysis for MIMO radar and telecommunication system coexistence
In *Proc. IEEE Int. Conf. Comput., Netw. Commun., Signal Process. Commun. Symp.*, 2014, pp. 534–539.

[24] A. Khawar, A. Abdelhadi, and T. C. Clancy
Target detection performance of spectrum sharing MIMO radars
IEEE Sensors J., vol. 15, no. 9, pp. 4928–4940, Sep. 2015.

[25] A. Khawar, A. Abdel-Hadi, and T. C. Clancy
MIMO radar waveform design for coexistence with cellular systems
In *Proc. 2014 IEEE Int. Symp. Dyn. Spectrum Access Networks: SSPARC Workshop*, McLean, VI, USA, Apr. 2014, pp. 20–26.

[26] A. Khawar, A. Abdelhadi, and T. C. Clancy
QPSK waveform for MIMO radar with spectrum sharing constraints, arXiv:1407.8510.

[27] F. H. Sanders, J. E. Carroll, G. A. Sanders, and R. L. Sole
Effects of radar interference on LTE base station receiver performance, U.S. Dept. Commerce, NTIA Rep. 14-499, May 2014.

[28] V. R. Cadambe and S. A. Jafar
Interference alignment and degrees of freedom of the K-user interference channel
IEEE Trans. Inf. Theory, vol. 54, no. 8, pp. 3425–3441, Aug. 2008.

[29] S. A. Jafar
Interference alignment: A new look at signal dimensions in a communication network
Found. Trends Commun. Inf. Theory, vol. 7, no. 1, pp. 1–134, 2011.

[30] C. Peel, B. Hochwald, and A. Swindlehurst
A vector-perturbation technique for near-capacity multiantenna multiuser communication—Part I: Channel inversion and regularization
IEEE Trans. Commun., vol. 53, no. 1, pp. 195–202, Jan. 2005.

[31] X. Shao, J. Yuan, and Y. Shao
Error performance analysis of linear zero forcing and MMSE precoders for MIMO broadcast channels
IET Commun., vol. 1, no. 5, pp. 1067–1074, Oct. 2007.

[32] A. Babaei, W. H. Tranter, and T. Bose
A practical precoding approach for radar/communications spectrum sharing
In *Proc. 8th Int. Conf. Cogn. Radio Oriented Wireless Netw.*, Jul. 2013, pp. 13–18.

[33] A. Khawar, A. Abdelhadi, and T. Clancy
Coexistence analysis between radar and cellular system in LoS channel
IEEE Antennas Wireless Propag. Lett., vol. 15, pp. 972–975, 2016.

Jasmin A. Mahal (SM'02–M'16) received the B.S. degree in electrical and electronic engineering from Bangladesh University of Engineering and Technology, Dhaka, Bangladesh, in 1998 and the M.S. degree in electrical engineering from Virginia Polytechnic Institute and State University, Blacksburg, VA, USA, in 2001, where she has been working toward the Ph.D. degree in electrical engineering since 2012.

Her research interests include physical layer security of LTE, MIMO communications, and spectrum sharing.

Awais Khawar received the B.S. degree in telecommunication engineering from the National University of Computer and Emerging Sciences, Peshawar, Pakistan, in 2007, the M.S. degree in electrical engineering from the University of Maryland, College Park, MD, USA, in 2010, and the Ph.D. degree in electrical engineering from Virginia Tech, Blacksburg, VA, USA, in 2015.

At the University of Maryland, his research focused on the security aspect of spectrum sensing in cognitive radio networks. His work on spectrum sensing security has featured in the IEEE COMSOC Best Readings in Cognitive Radio. At Virginia Tech, his research focused on spectrum sharing, security, optimization, and resource allocation for coexisting wireless communication and radar systems. He is the author of the books *MIMO Radar Waveform Design for Spectrum Sharing With Cellular Systems* (Springer-Verlag, 2016) and *Spectrum Sharing Between Radars and Communication Systems* (Springer-Verlag, 2017).

Ahmed Abdelhadi (SM'16) received the Ph.D. degree in electrical and computer engineering from the University of Texas at Austin, Austin, TX, USA, in December 2011.

He is currently a Research Assistant Professor at Virginia Tech, Blacksburg, VA, USA. He was a member in Wireless Networking and Communications Group during his Ph.D. From 2012 till June 2016, he was a Postdoctoral Associate, then a Research Scientist in the Bradley Department of Electrical and Computer Engineering and the Hume Center for National Security and Technology at Virginia Tech. His research interests include the areas of wireless communications and networks, spectrum sharing, radar systems, and security.

T. Charles Clancy (M'05–SM'10) received the B.S. degree in computer engineering from the Rose-Hulman Institute of Technology, Terre Haute, IN, USA, in 2001, the M.S. degree in electrical engineering from the University of Illinois, Champaign, IL, USA, in 2002, and the Ph.D. degree in computer science from the University of Maryland, College Park, MD, USA, in 2006.

He is currently an Associate Professor of electrical and computer engineering at Virginia Tech, Blacksburg, VA, USA, and directs of the Hume Center for National Security and Technology. Prior to joining Virginia Tech in 2010, he was a Senior Researcher at the Laboratory for Telecommunications Sciences, a defense research lab at the University of Maryland, where he led research programs in software-defined and cognitive radio. He has more than 150 peer-reviewed technical publications. His current research interests include cognitive communications and spectrum security.